SKB

TECHNICAL REPORT 98-06

Indications of uranium transport around the reactor zone at Bagombe (Oklo)

I Gurban[1], M Laaksoharju[1], E Ledoux[2], B Made[2], A L Salignac[2]

1 Intera KB, Stockholm, Sweden
2 Ecole des Mines, Paris, France

August 1998

SVENSK KÄRNBRÄNSLEHANTERING AB
SWEDISH NUCLEAR FUEL AND WASTE MANAGEMENT CO

P.O.BOX 5864 S-102 40 STOCKHOLM SWEDEN
PHONE +46 8 459 84 00
FAX +46 8 661 57 19

INDICATIONS OF URANIUM TRANSPORT AROUND THE REACTOR ZONE AT BAGOMBE (OKLO)

I Gurban[1], M Laaksoharju[1], E Ledoux[2], B Made[2], A L Salignac[2]

1 Intera KB, Stockholm, Sweden
2 Ecole des Mines, Paris, France

August 1998

INDICATIONS OF URANIUM TRANSPORT AROUND THE REACTOR ZONE AT BAGOMBE (OKLO)

I. Gurban[1)], M. Laaksoharju[1)], E. Ledoux[2)], B. Made[2)], Salignac, A.L.[2)]

[1)] INTERA KB, STOCKHOLM

[2)] ECOLE DES MINES, PARIS

Keywords: Natural Analogue, Coupled Code, Statistical-Mathematical Code, Uranium Transport, Hydrodynamic and Geochemical Modelling

ABSTRACT

Swedish Nuclear Fuel and Waste Management Company (SKB) is responsible for the safe handling and disposal of nuclear wastes in Sweden. This responsibility includes conducting studies into the siting of a deep repository for high-level nuclear waste. The aim of this study is to use the hydrogeological and hydrochemical data from Oklo Natural Analogue to compare the outcome of two independent modelling approaches (HYTEC-2D and M3) which can be used to model natural conditions surrounding the reactor.

HYTEC-2D represents a 2D, deterministic, transport and multi-solutes reactive coupled code developed at Ecole des Mines de Paris. M3 (named Multivariate Mixing and Mass balance calculations) is a mathematical-statistical concept code developed for SKB. The M3 results are visualised using the Voxel Analyst code and the outcome of the uranium transport predictions are made from a performance assessment point of view.

This exercise was in the beginning intended to represent a validation for M3, by comparing this statistic approach with the standard hydrodynamic- geochemical coupled code HYTEC-2D. It was realized that the codes complete each other and a better understanding of the geochemical studied system is obtained. Thus, M3 can relatively easily be used to calculate mixing portions and to identify sinks or sources of element concentrations that may exist in a geochemical system. This can help to address the reactions in the coupled code such as HYTEC-2D, to identify the hydrodynamic and hydrochemical system and to reduce the computation time.

M3 shows the existence of the buffer around the reactor (sampling campaign 1993). No transport of uranium was indicated downstream the reactor. HYTEC-2D gives the same result in the case when we consider the existence of the redox buffer in the model. M3 shows an increase of the alkalinity in the reactor zone. The increase of the alkalinity was indicated by the M3 modelling to be associated with microbial decomposition of organic material which added reducing capacity to the system. The modelling result was supported by new results from the last field campaign, which included in-situ Eh measurements and microbial sampling and identification. The effects from the same process was indicated also by the HYTEC-2D predictions which show an increase of the pH in the reactor zone, due to the existence of the buffer. The two modelling approaches can be used to complete each other and to better understand the processes that can take place in nature. Thus, we can build confident tools which can be used to support performance assessment.

ABSTRACT (SWEDISH)

Svensk Kärnbränslehantering (SKB) ansvarar för hantering och lagring av använt kärnbränsle i Sverige. Utförandet av studier för placering av djupförvar av högaktivt kärnavfall ingår i detta ansvarstagande. Målet för denna studie är att använda hydrogeologiska och hydrokemiska data från det naturliga analoga programmet i Oklo, Gabon. Syftet var att jämföra resultaten av två oberoende modeller, HYTEC-2D och M3, vilka kan användas för att modellera naturliga förhållanden runt förvaret.

HYTEC-2D representerar en 2D, deterministisk, transport och reaktivt kopplad modell, utvecklad vid Ecoles des Mines i Paris. M3 (Multivariat Blandnings- och Massbalans-beräkningar) är en matematisk statistisk modell, utvecklad för SKB. M3 resultaten har visualiseats med Voxel Analyst modellen och resultaten av urantransportmodelleringen är gjord från en säkerhetsanalys synvinkel.

Denna uppgift var i början menad att representera en utvärdering av M3 modellen, genom att jämföra det statistiska närmandet med en standardiserad hydrodynamisk – geokemisk kopplad modell som HYTEC-2D. Det visade sig att modellerna kompletterade varandra och en ökad förståelse av det undersökta geokemiska systemet har erhållits. M3 kan relativt lätt användas för att beräkna blandningsproportioner och för att identifiera förlust och tillskott av elementhalter som kan förekomma i ett geokemiskt system. M3 resultaten kan underlätta identifieringen av reaktioner som kan simuleras i HYTEC-2D samt för att identifiera hydrogeologiska- och geokemiska system och för att därmed minska beräkningstiden.

M3 modelleringen visar närvaro av buffring kring reaktorn (provtagningskampanj 1993). Ingen transport av uran ses nedströms reaktorn. HYTEC-2D ger samma resultat i det fall där hänsyn tas till närvaro av en redoxbuffer i modellen. M3 visar en ökning av alkaliniteten i reaktorzonen. Denna ökningen av alkaliniteten är assosierad med mikrobiologisk nedbrytning av organiskt material vilket bidrar till den reducerande kapaciteten i systemet. Modelleringsresultaten stöds av nya resultat från den senaste provtagningskampanjen, vilket inkluderar in-situ Eh-mätningar och mikrobiologisk provtagning och identifiering. Effekten från samma process indikeras också av HYTEC-2D modelleringen vilken visar en ökning av pH i reaktorzonen, orsakad av närvaro av en buffert. De två modelleringsätten kan användas för att komplettera varandra och för att bättre förstå processerna som kan ske i naturen. Ett säkert verktyg kan därför skapas, vilken kan användas som stöd för säkerhetsanalyser.

TABLE OF CONTENTS

LIST OF FIGURES

1 INTRODUCTION

Swedish Nuclear Fuel and Waste Management Company (SKB) is responsible for the safe handling and disposal of nuclear wastes in Sweden. This responsibility includes conducting studies into the siting of a deep repository for high-level nuclear waste. This report compares two different modelling approaches as part of a performance assessment (PA) study of the long-term safety of a natural repository (Oklo).

SKB is conducting and participating in Natural Analogue activities as part of various studies regarding the final disposal of high level nuclear waste (HLW). The aim of this study is to use the hydrogeological and hydrochemical data from Oklo Natural Analogue to compare the outcome of two independent modelling approaches which can be used to predict the repository performance over long periods of time.

The Oklo site is a unique analogue for the source term such as uraninite versus spent fuel and the engineered and geological barriers (clay minerals, apatite). This provides an opportunity to assess the necessary tools for future performance assessment of the prospective real waste repository sites.

2 PROJECT DESCRIPTION

The work presented in this study was performed as a collaboration between Ecole des Mines de Paris and Intera KB.

The natural analogue project in Bangombé concerns groundwater modelling based on existing data. The aim is to use different computer methodologies to characterise the evolution of the groundwater system and its implications in radionuclide transport, and then to compare and integrate the results within a performance assessment concept concerning uranium transport from the source to the biosphere. Thus, the modelling helps to evaluate the processes associated with nuclear natural reactors such as redox, adsorption– desorption and dissolution–precipitation of the uranium and to develop more realistic codes used in performance assessment studies.

3 TOOLS

Two approaches were used: a classic one, representing a coupled hydro-geo-chemical transport code developed at Ecole des Mines de Paris named HYTEC-2D and a new concept code named M3 developed for SKB. The M3 results are visualised using the Voxel Analyst code and the outcome of the uranium transport predictions are made from a performance assessment point of view.

3.1 HYTEC2D DESCRIPTION

The 2D, deterministic, transport and multi-solutes reactive code named HYTEC2D (Salignac, 1997 and 1998) is the result of combining the solute transport code METIS (Cordier and Goblet 1996, Goblet 1981 and 1989) and the chemical speciation code CHESS (Van der Lee, 1993 and 1997) developed at Ecole des Mines. It allows the computation of the chemical composition of the groundwater through a heterogeneous geological system taking into account the interaction between fluid and rock due to precipitation-dissolution, gas formation, ion exchange, and surface complexation. This model was applied to the Bangombé geochemical system in the vicinity of the reactor zone as regards the mixing of a deep water flowing through sandstones (borehole BAX05) and of a shallow water flowing through the overburden of pelites (borehole BAX06). The results are expressed in terms of distribution in space and time of the aqueous, solid or gaseous species, of the saturation index versus minerals that may control the geological system and of the mass balance between fluid, solid and gas. Several hypotheses for the control of dissolved uranium can thus be tested and compared to the experimental database.

These results were then compared to the M3 analysis results expressing the chemical tendencies.

3.2 M3 DESCRIPTION

The origin and evolution of the groundwater can be described if the effect from mixing and reactions can be examined separately. In order to do this separation a new method named Multivariate Mixing and Mass balance calculations (abbreviated to M3) was constructed (Laaksoharju *et. al.*, 1997 and 1998). The model consists of 3 steps where the first step is a standard principal component analysis, followed by mixing, and finally by mass balance calculations. Mass balance calculations are used to define the sources and sinks for different elements, which deviate from the ideal mixing model used in the mixing calculations. The mixing portions are used to predict new values for the elements. No deviation from the measured value indicates that mixing can explain the element behaviour. A source or sink is due to mass balance reactions. M3 uses the opposite approach to that of other standard methodologies. In M3 the mixing processes are evaluated and calculated first. The constituents that cannot be described by mixing are described by reactions. M3 computer code determines

the origin of the water, the mixing proportions and the most important mass balance reactions that take place in the groundwater.

3.3 VOXEL ANALYST

In order to compare the results, the Voxel Analyst computer code was used to visualise the M3 results. Voxel Analyst is a general-purpose data visualisation and analysis tool that helps to understand the relationship between different attributes within a 3-dimensional volume data set.

The outcome of the modelling is interpolated, visualised and compared by Voxel Analyst. The major flow-paths and reaction paths were identified and used for transport evaluation.

4 MODELLED AREA

The geological cross-section produced by the conceptual model and the collected data were used as a basis for two-dimensional, local-scale modelling (Gurban, 1996, Toulhoat et. al. 1994). The model domain corresponds to a vertical cross-section between BAX01 and BAX07. The lower boundary of the model is located at 300 m above sea level while the upper one varies with the topography between 406.8 m and 378.6 m above sea level. This cross-section is used as support for the modelling with M3. HYTEC is applied on a limited area, around the reactor (figure 4.1).

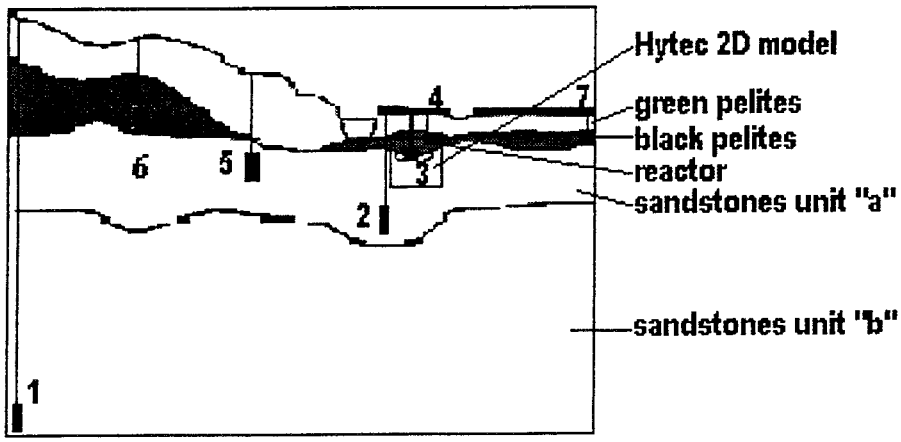

Figure 4.1 *Modelled profile for M3 and HYTEC-2D, boreholes location, geological structure.*

The hydrodynamic boundary conditions for this model are extracted from the Gurban et. al. (figure 4.2, a).

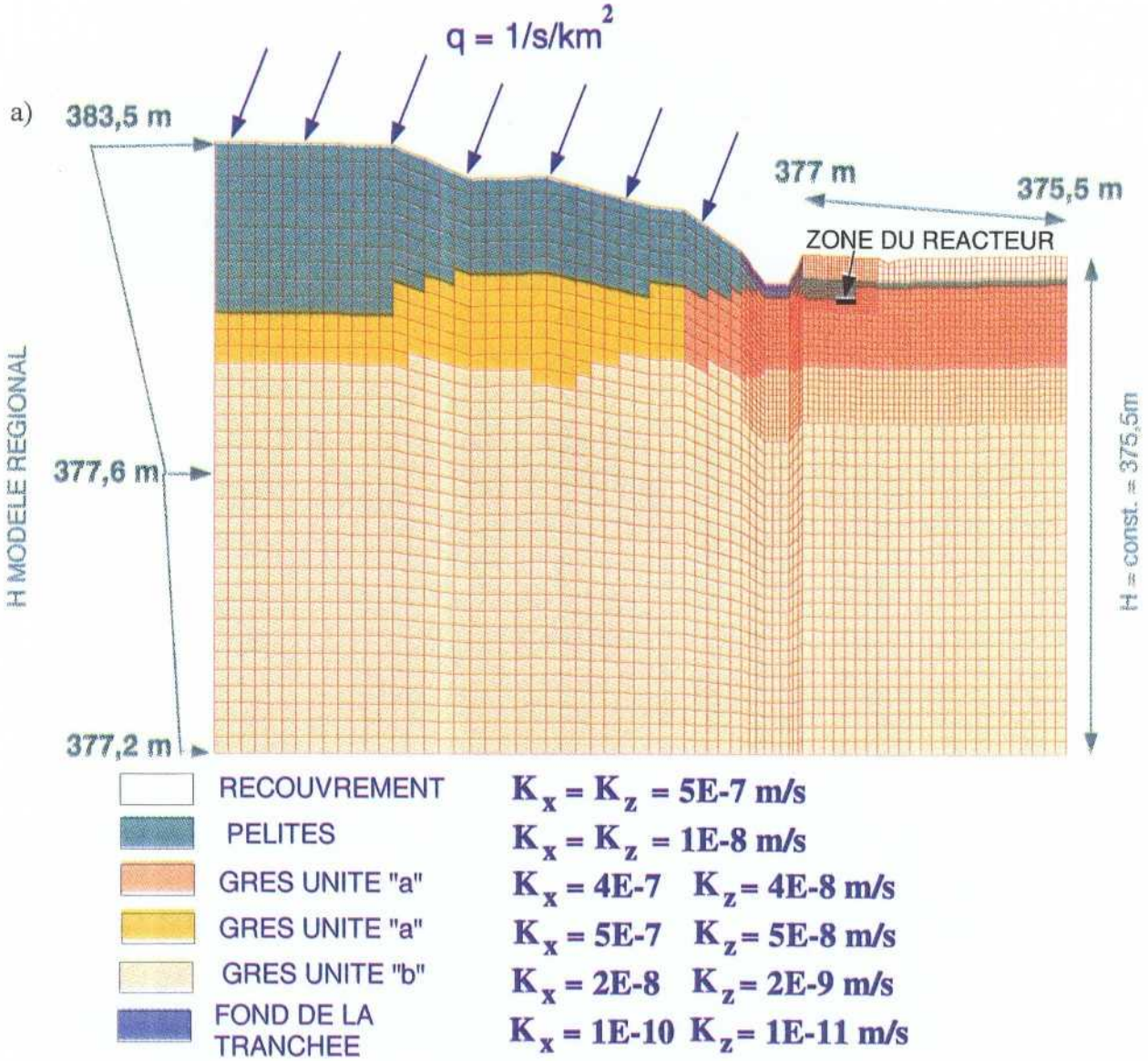

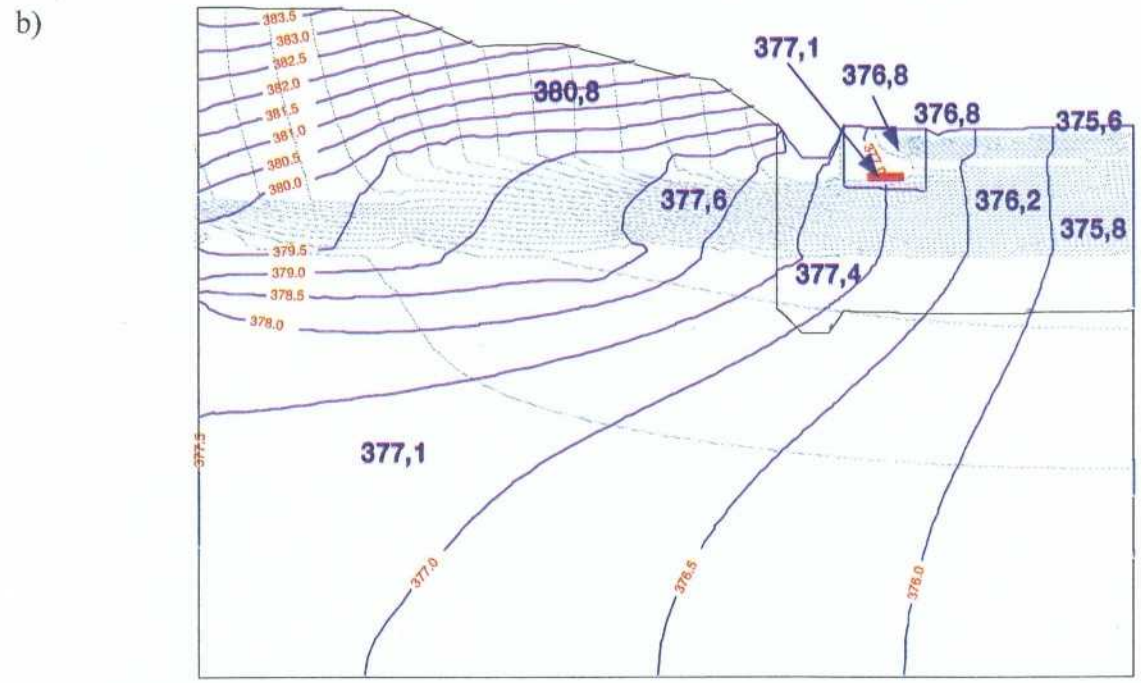

Figure 4.2 *a) Mesh used for the modelled area, boundary conditions and hydraulic properties. b) Isopotential and flow map (from Gurban et al. 1996).*

5 HYTEC2D MODELLING

5.1 HYTEC2D APPROACH

Two major processes take place in the aquifer: transport due to advection, diffusion and dispersion and chemical reactions, into the aqueous phase and at the interface of the solid matrix. Each of these processes is complex enough to require numerical models. Ecole des Mines has developed a speciation static code CHESS for the modelling of the geochemistry, and the code METIS for the transport. Combining the two codes, Ecole des Mines obtained a 2D transport multi-solute reactive code named HYTEC-2D. This code works in heterogeneous saturated media and allows the hydrodynamic parameters and the chemical conditions defining the system to regionalise. This code is based on the algorithm named "two-steps" iteractive. It means that the chemical and transport calculations are made sequentially by two distinct moduls.

a) The *chemical model CHESS* enables the speciation within a geochemical system in the hypothesis of local chemical equilibrum to be calculated using the thermodynamic constants of the assumed reactions. It takes into consideration the method of the base components, considering the system as a vectorial space where a base is chosen. If species (N_{es})are correlated by independent reactions (N_r), is defined $N_{co}= N_{es}-N_r$, named base components and represents the unknowns. To solve the N_{co} equations system, the law of mass action and conservative mass balance law are used.The resulting equations are strongly non-linear. The iterative Newton Raphson method is used to solve them.

b) The *hydrodynamic model METIS* by finite element method enables a steady state flow to be calculated combined with a transient transport of chemical species, in a saturated medium, monophasic and bidimensional.

c) *HYTEC2D combination*
The two systems of equations are very different:
- the chemical equations are independent in space (the speciation is calculated step by step), and the transport equations are solved simultanously in all the domains.
- The chemical equations are solved for all the base components simutaneously, but the transport equations are independent in this respect.
- The chemistry is not dependent on time (local equilibrium), but the transport is dependent on time.

The numerical solution method of the coupled geochemistry-transport model, HYTEC-2D, includes, for each time step, a two-step iterative sequence where the first step is the speciation calculation on all the elements of the domain and the second one is the solute transport calculation. As local equilibrium is assumed, the chemical reactions are instantaneous. Only the base components are transported. The concentrations of the secondary species are known at each step from the speciation calculations. The transport equation used here is that of advection-diffusion, using as variable the total concentration of the components, representing changes (gains or losses), during a time step, for the relevant solute species. This two-step

approach is iterative in that, at the end of the transport step, we check that the condition of equilibrium at all points is always respected.

5.2 PRELIMINARY ASSUMPTIONS

The preliminary assumptions for the coupled hydrodynamic– geochemical HYTEC-2D modelling are as following (Gurban et al, 1996):

The rock matrix found around the reaction zone is rich in organic matter and may act as a buffer zone against atmospheric oxygen. This suggests that a reducing matrix protects the uraninite from being dissolved through oxidation. The exact location of the reducing matrix, acting as a redox buffer, is unknown but a sharp variation in space of the redox conditions is assumed to occur above BAX02 and between BAX05 and BAX04. Consequently, the role of the redox buffer (Eh = 26mV) protecting the reactor zone can be represented by two geochemical systems:

1) the organic matter, abundant in the reactor zone and represented by graphite. The hydrolysis of graphite generates methane and carbon dioxide. Methane combined with gaseous oxygen and carbon dioxide combined with water produce dissolved bicarbonates. According to Nagy (1993), the graphite seems to play an additional role of ``physical protection" of the reactor in spite of its hydrochemical and redox properties. A more or less diffuse graphite matrix in the zone containing the uraninite, would protect it since the graphite is impervious to water and highly corrosion resistant. However, in this case the medium appears to be fairly permeable to water as demonstrated by the hydrogeology study. Therefore, the very slow kinetics of the graphite might be thought more likely to limit the effectiveness of the buffer.

2) a system represented by two iron minerals used to define and constrain the redox couple Fe^{2+}/Fe^{3+} in the water. The minerals chosen to represent the redox buffer are siderite, $FeCO_3$, for ferrous iron and ferrihydrite, $Fe(OH)_3$, for ferric iron.

This reducing matrix protects the uraninite in the reaction zone from potential dissolution by the relatively oxidizing water whose chemical composition is represented by borehole BAX05. These two systems, organic matter and iron minerals, acting as a redox buffer, might coexist in the matrix. There is an abundance of organic matter (Bros et al., 1993), however for groundwater, the kinetics of the Fe^{2+}/Fe^{3+} couple are fast and therefore more likely to condition the value of the redox potential. Thus, the system chosen in HYTEC-2D modelling to control the redox buffer is based on the Fe^{2+}/Fe^{3+} couple, represented by siderite and ferrihydrite respectively and the mechanism is strengthened by the presence of organic matter.

5.3 HYTEC-2D MODELLING SETTINGS

The dilution was calculated with METIS over the entire local scale model domain. The results were then used to extract the boundary conditions for flow to sub-domain located around the reactor zone. This sub-domain was used in the HYTEC simulations and includes the unit "a" sandstone, parts of the pelite situated above the BAX04 borehole, the reactor and the buffer (figure 5.1). The heterogeneity of the system is taken into account in the assignment physical

parameters, for transport, and in the values of the redox potential in each of the rocks, for the geochemistry (Madé and Salignac, 1998).

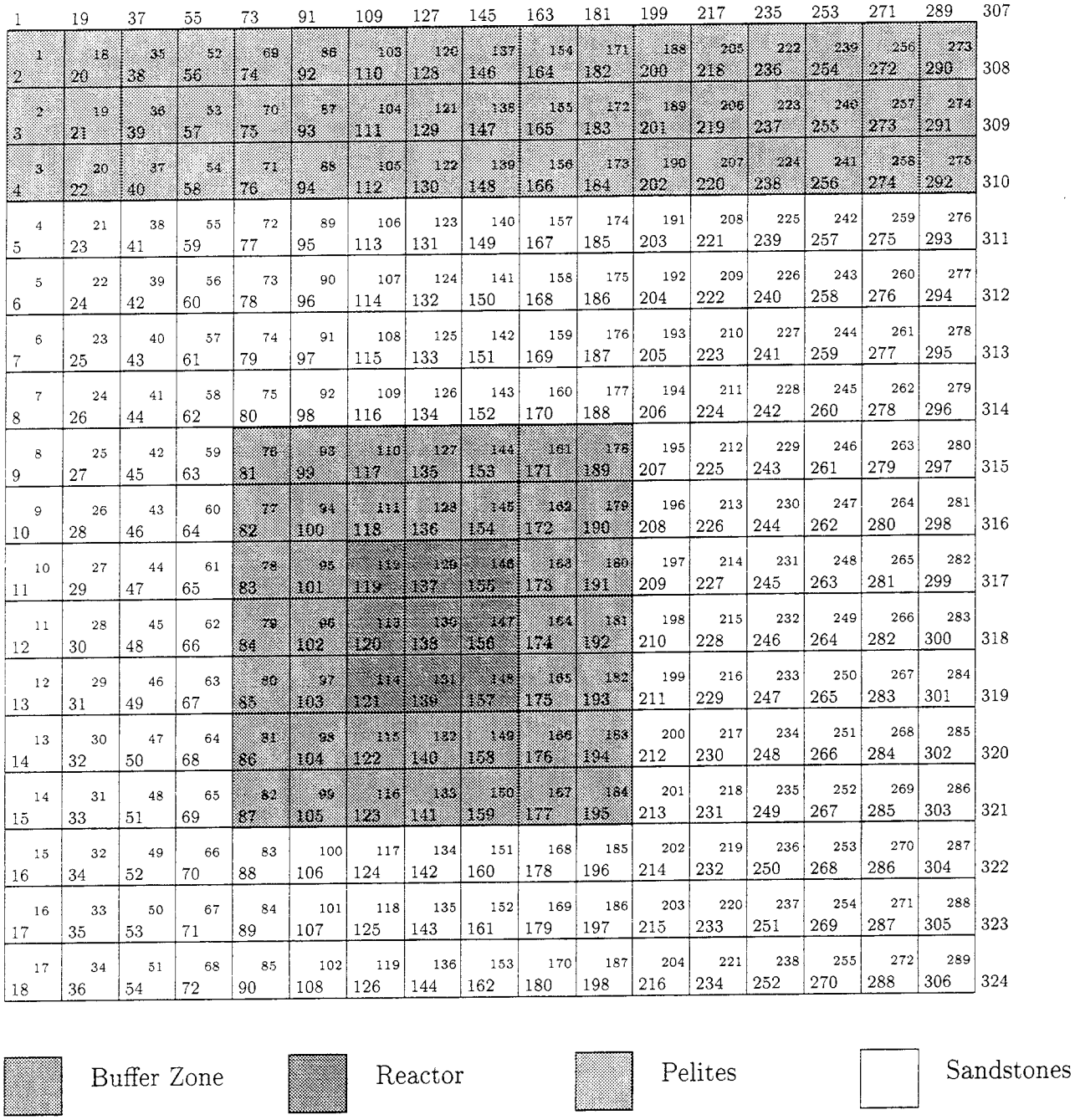

***Figure 5.1** Mesh used for HYTEC-2D modelling*

The boundary conditions are as follows:

- The downstream boundary of the model represents the outlet of the domain
- Prescribed head, along the upstream vertical boundary, at the bottom and at the surface of the local model domain, obtained from the regional model (Gurban et. al).

Figure 4.2, b) shows the stream lines generated by these geological and boundary conditions.

Physical parameters

- Porosity: constant and uniform, 1 %.
- Longitudinal and transversal dispersivities and the diffusion coefficient are constant and uniform, equal to 5m, 2m and $10^{-7}m^2/s$.
- Permeability:

$K_x = 4x10^{-7}$ and $K_y = 4x10^{-8}$ m/s for the sandstones and the buffer
$K_x = K_y = 10^{-8}$ m/s for the pelites and the reactor

Selection of the relevant data

Water from the March 1993 exercise was chosen as a basis for the modelling because its ion analyses and, above all, its electrical equilibrium were found to be better than analyses from other campaigns.

Chemical data-base

The 13 base components representing the chemistry in the modelling are:

$O_2(aq)$, H^+, UO_2^{2+}, SO_4^{2-}, Cl^-, Ca^{2+}, K^+, Mg^{2+}, Na^+, HCO_3^-, Fe^{2+}, $SiO_2(aq)$, Al^{3+}.

From these base components, 117 chemical species (aqueous and gaseous) are generated and 55 minerals. The aqueous complexation reactions, redox reactions and precipitation/dissolution reactions were particularly investigated. The sorption on the surface minerals and the colloids were ignored at this stage of the modelling.

Different chemical areas

Four distinctive areas are identified as a function of the spatial variability chemistry and mineralogy (Fig. 5.1).

Area 1 - the sandstones: domain in equilibrium with Chalcedony. The chemical composition of the aqueous solution is given by the borehole BAX05 (pH = 6.57 and Eh = 147 mV).

Area 2 - the pelites: domain in equilibrium with Chalcedony (concentration of silica) and illite (concentration of Aluminium). The chemical composition of the aqueous solution is given by the surficial borehole BAX06 (pH = 5.64 and Eh = 277 mV).

Area 3 - the reactor: domain in equilibrium with Chalcedony, "argile de pile" (chemical composition in Gauthier-Lafaye, 1986) and Uraninite (concentration of uranium). The chemical composition of the aqueous solution in the reactor zone is given by the borehole BAX03 (pH = 6.69 and Eh = 26 mV).

Area 4 - the redox buffer: domain in equilibrium with Chalcedony and two iron minerals controlling the redox conditions; Siderite (ferrous carbonate) and Ferrihydrite (ferric hydroxide). The chemical composition of the aqueous solution in the redox buffer zone is given by the borehole BAX05 but with the uranium concentration in equilibrium with respect to Uraninite at Eh = 135 mV.

The chemical boundary conditions are imposed concentrations (on nodes) at the boundaries of geometrical system (upstream, top and bottom). On the rest of the spatial domain (on others nodes), the physico-chemical conditions described above are used as initial conditions.

In order to identify the real system, several types of simulations were studied (Madé and Salignac, 1998):

case 1: without precipitation of secondary minerals and without redox buffer zone;

case 2: with precipitation of secondary minerals and without redox buffer zone;

case 3: without precipitation of secondary minerals and with redox buffer zone;

case 4: with precipitation of secondary minerals and with redox buffer zone.

In the cases where the precipitation of secondary minerals are permitted [case 2 and case 4], the aqueous distribution of uranium around the reactor zone is similar if the redox buffer zone is considered or not. For the case 2, the Eh value in the reactor zone increases from 26 to 60 mV, the pH decreases from 6.69 to 6.6 and the aqueous concentration of uranium is equal to $1.2x10^{-9}$ mol/l. This concentration is controlled by the equilibrium with respect to a secondary mineral UO2.25 (mineral Uiv - Uvi). For the case 4, a part of the redox buffer zone is destroyed characterised by the Siderite dissolution. The Eh value in the reactor zone increases from 26 to 40 mV, the pH from 6.69 to 6.86. This increasing of pH value can be connected with the Siderite dissolution releasing bicarbonate ions (HCO_3^-). The aqueous concentration of U is similar with this of case 2 controlled by the equilibrium with mineral UO2.25 (tot U(aq) = $1.25x10^{-9}$mol/l). In the redox buffer zone, an additional equilibrium between Magnetite/Nontronite or Daphnite-14A/Cronstedtite-7A take the place of Siderite/Ferrihydite equilibrium. It means that the precipitation of secondary phases of U (as UO2.25 and Uraninite) has a higher impact on the uranium behaviour than the buffer zone.

Only the case without precipitation of secondary minerals will therefore be discussed below (case 1 and case 3).

The simulation procedure is as follows: waters with the same aqueous chemical composition as that in BAX05 (Eh initial = 147 mV) and in BAX06 (Eh initial = 277 mV) percolate in the spatial domain modelled. The coupled chemical reactions-transport code HYTEC-2D (Salignac, 1998) can superimpose geochemical phenomena on dilution. Transport of the aqueous uranium downstream the reactor is observed.

For the case 1, the pH value in the sandstone and in the reactor zone (Fig 5.2) is uniform and close to the pH of the borehole BAX05 (pH = 5.7). The Eh value in the reactor zone increase

from 26 to 100 mV. The total aqueous concentration of uranium in the reactor zone is equal to $9.9x10^{-8}$ mol/l (Fig. 5.3).

When we consider the presence of a redox buffer zone, the water reaches equilibrium with respect to specific solid phases Siderite ($FeCO_3$) and Ferrihydrite ($Fe(OH)_3$). These phases act as a "redox buffer" maintaining an Fe^{2+}/Fe^{3+} equilibrium in the aqueous solution. This matrix protects the uraninite in the reaction zone from potential dissolution by oxidizing water (chemical composition of borehole BAX05). An increase of the pH is observed downstream the reactor (Fig. 5.2) varying in the sandstone from 6.6 to 6.8 and varying in the reaction zone from 6.69 to 6.86. This increasing of pH is consistent with the Siderite dissolution of the redox buffer zone (aqueous concentration of HCO_3^- increases). The Eh value in the reactor zone change from 26 to 100 mV. In the buffer zone in front of reaction zone, the Eh increases from 135 to 147 mV. Behind the reactor, the Eh describes a reductive plume.

The total aqueous concentration of uranium in the reaction zone increase from $8.4x10^{-10}$ mol/l (tot U(aq) in equilibrium with Uraninite at 26 mV) to $5.7x10^{-7}$ mol/l (tot U(aq) in equilibrium with Uraninite at 100 mV). On the figure 5.3, the impact of the redox buffer zone on the uranium transport can be observed. Thus, a diminution of the uranium transport downstream the reactor is observed (Fig. 5.3). This plume of depleted uranium can be explain the anomaly ratio $^{235}U/^{238}U$ characterizing an isotopic signature from the reactor zone.

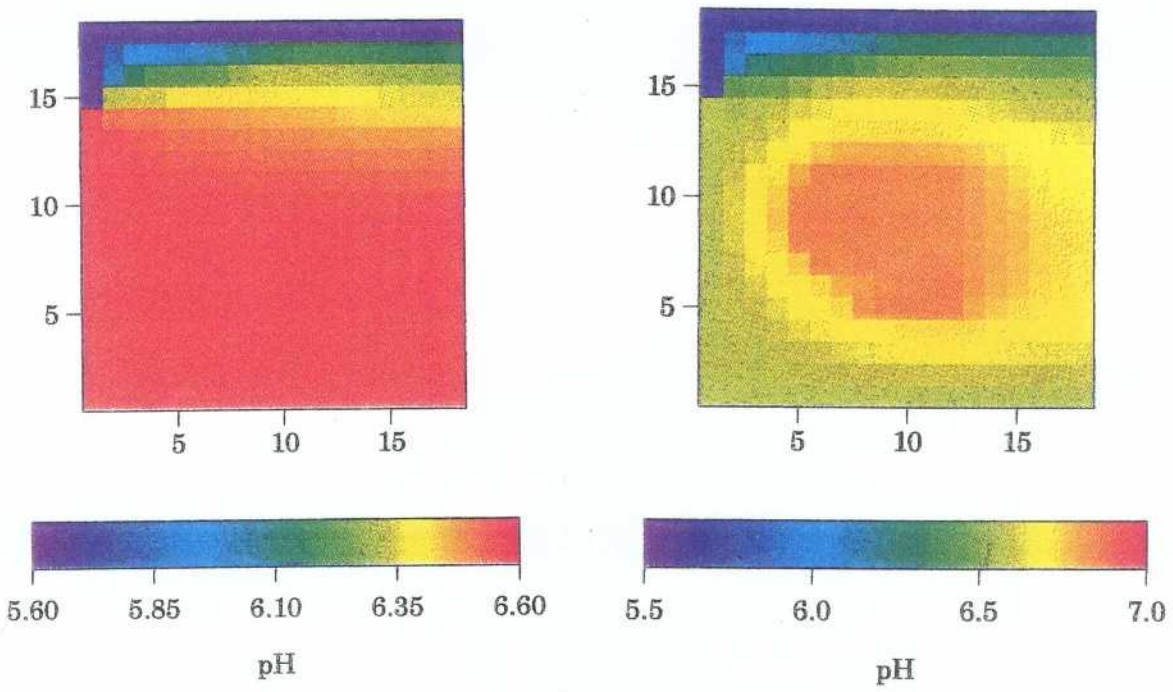

Figure 5.2 *Evolution of the pH around the reactor zone (t=3.17 years). To the left, the evolution of the pH without buffer, to the right, the evolution of the pH with buffer.*

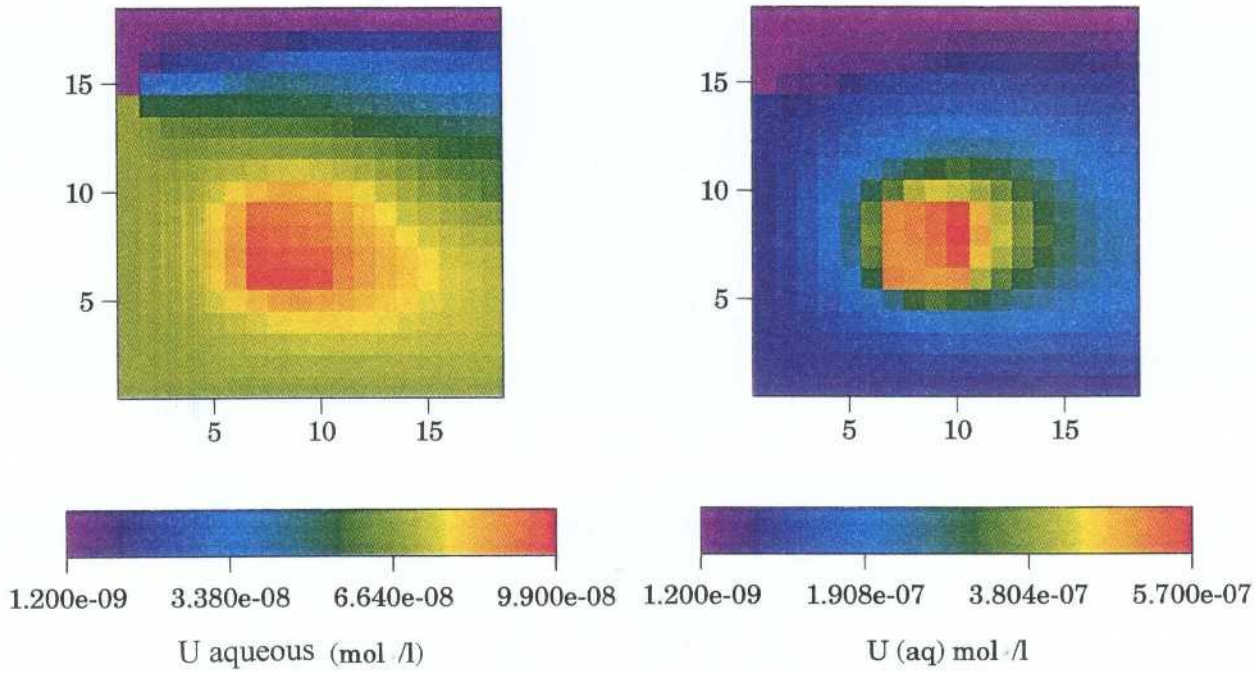

Figure 5.3 *Evolution of the aqueous uranium concentration (mol/l) around the reactor zone (t=3.17 years). To the left, the evolution of the uranium concentration without buffer, to the right, the evolution of the uranium concentration with buffer. The concentration of uranium is generally higher for the case when the buffer is considered. This is probably due to the effects of carbonate in the system increasing the solubility of U.*

6 M3 MODELLING

6.1 METHOD DESCRIPTION

Many variables and different sampling campaigns are important for the understanding of the natural system. The information gathered in many variables can be handled using multivariate techniques.

The origin and evolution of the groundwater can be described if the effect from mixing and reactions can be examined separately. In order to do this separation a new method named Multivariate Mixing and Mass balance calculations (abbreviated to M3) was constructed (Laaksoharju et al., 1995; Laaksoharju and Skårman, 1997). The model consists of 3 steps where the first step is a standard principal component analysis, followed by mixing, and finally by mass balance calculations according to:

1. A standard multivariate technique called Principal Component Analysis (PCA) which is used for the clustering of the data using the major components Cl, Ca, Na, Mg, K, SO_4 and HCO_3. PCA aims to describe as much of the information from the ten variables in the first equation (called the first principal component) as possible. As much as possible of the remaining information is described by the second principal component. The principal components are equations of linear combinations that describe most of the information in the data. The weights for the different variables in the equations are calculated automatically by the PCA. For the Bangombé data set the first two principal components can be used to describe 66% of the information in the data set. The third or fourth principal components generally do not contain useful information but this is dependent on the complexity of the examined data and the chosen variables. If the first two principal components contain most of the information, an x, y scatter plot can be drawn. The x is the equation for the first principal component and y the equation for the second principal component. The plot is named the M3 plot and is used to visualise the clustering of the data as well as to identify extreme waters. Extreme waters can be an end-member composition such as rain water, deep water or intermediate water (see figure 6.1). Lines are drawn between the extreme waters so a polygon is formed. The polygon defines the observations, which can be described by the selected extreme waters. By definition the selected extreme waters can describe the observations inside the polygon. The groundwater composition of an observation inside the polygon is compared to the chosen extreme water compositions.

2. Mixing calculations are used to calculate the mixing portions. The mixing portions describe the contribution of the end-member to the observed water. The calculated mixing portion can be used to describe the origin of the groundwater. The mixing portions are equal to the distance to the selected reference waters or end-members in the M3 plot (see figure 6.1). From a two-dimensional surface, mixing portions containing a maximum of three reference waters can be calculated so that a mathematically unique solution is obtained. To avoid this shortcoming and to be able to use if necessary more than three reference waters in the model a control point with a known mixing portion was added to the calculations. A polygon containing say five reference waters contains a portion of 25% of each reference water in the centre point. By using this

addition a mathematically unique solution can be achieved from a two dimensional plane with more than three reference waters (Laaksoharju et al., 1998). A mixing portion calculation of less than 10% is regarded as under the detection limit for the M3-method and is therefore uncertain.

3. Mass balance calculations are used to define the sources and sinks for different elements which deviate from the ideal mixing model used in the mixing calculations (see Figure). The mixing portions are used to predict new values for the elements. No deviation from the measured value indicates that mixing can explain the element behaviour. A source or sink is due to mass balance reactions. The evolution of the groundwater can thus be described.

The M3 model can describe the origin and evolution of the groundwater chemistry by means of the major mixing processes and mass balance reactions. It is important to note that the modelling is always relative to the selected reference waters or end-members. The modelling constraints can be changed depending on the selection of extreme waters. It is important to note that the M3 model deals only with chemical information; no space or time constraints are included in the model.

Back-propagation tests where 400 given mixtures of groundwaters were modelled using the M3 concept show that the accuracy of the mixing calculations is generally ±10.5% (Laaksoharju and Wallin (Eds.), 1997). Small errors in the prediction of conservative element behaviour may lead to large errors in the mass balance calculations. A low resolution may lead to difficulties in identifying the end-members and in correctly modelling the system.

6.2 REFERENCE WATERS

The PCA plot is a useful tool to examine the variability and the origin of the groundwater and to choose the end-members in relation to the hydrodynamic model made by Gurban et. al. (figure 6.1).

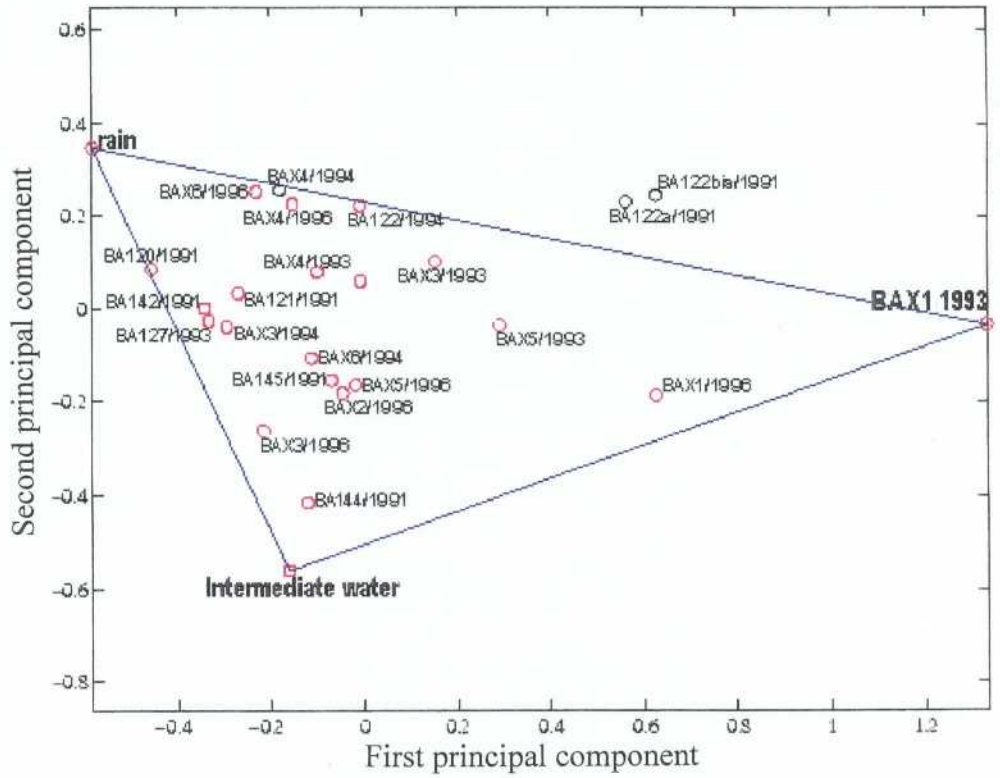

Figure 6.1 *PCA plot, identification of the samples, end-members. The first and second principal components are based on the following chemical constituents: alkalinity, Cl, SO_4, Na, K, Ca, Mg, and U.*

6.3 SELECTION OF THE END-MEMBERS FOR THE M3 MODELLING

The selected end-members for the current modelling are shown in figure 6.1 in relation to the sampled groundwaters at Bangombé. The ID codes for the chosen reference waters are shown. The end-members were selected so that the samples can be described. The criteria are by definition that a sample inside the polygon can be described by the selected end-members. The closer to the end-member a groundwater observation plots in PCA the more of that end-member the water contains. The reason for modelling all the campaigns simultaneously by using the same end-members is that we can obtain the maximum amount of information about the whole system and at the same time compare the evolution of the geochemistry.

The analytical data for the end-members are listed in Appendix 1. The selected end-members for M3 Bangombé modelling are:

- **Meteoric: corresponding to the precipitation and infiltration water (see Appendix 1 row 26);**
- **Deep water: described by BAX01 (see Appendix 1, row 11);**
- **Intermediate water: described by BAX05 (see Appendix 1 row 27).**

The latest findings (Pedersen and Karlsson, 1995) indicate that the biological processes play an important role in mediating reactions in groundwater, by regulating the redox conditions around the reactor. The following biological processes were modelled using M3:

Table 1

- Oxygen consumption through oxidation of organic matter
  $O_2 + (CH_2O) \rightarrow CO_2 + H_2O$

- Reduction of iron(III) minerals through oxidation of organic matter
  $4Fe(III) + (CH_2O) + H_2O \rightarrow 4Fe^{2+} + 4H^+ + CO_2$

- Reduction of sulphate through oxidation of organic matter
  $SO_4^{2-} + 2(CH_2O) + H^+ \rightarrow HS^- + 2H_2O + 2CO_2$

During the last field campaign (Karsten Pedersen et al. March, 1998) the microbes were sampled and identified in and around the reactor. Large amounts of iron reducing microbes, organic matter but no sulphate reducing microbes were detected at the Bangombé site.

6.4 3D VISUALISATION OF THE M3 CALCULATIONS

In order to visualise the distribution of uranium, alkalinity, calcium, sulphate and Cl and the results of the mixing portion calculations of rain, deep water and intermediate water, a 3D interpolation was performed using Voxel Analyst by INTERGRAPH.

The vertical cross-section from BAX01 to BAX07 was selected to show the distribution of the salinity and dominating water types, alkalinity, Ca, SO_4 and uranium, and this also reflects the specific geological structures. The geological structures are from top to bottom: green pelites, black pelites (shown in grey on the figures 6.2 to 6.11), sandstones unit "a" and sandstones unit "b".The boreholes BAX01 to BAX07 are shown in figures 6.2 to 6.11.

The modelling is based solely on chemical information which can be used to support the 3-D understanding of groundwater flow through the site area. The calculated mixing portions are always relative to the selected end-members. The distribution of the chosen major elements, salinity and uranium in portions of rain, deep and intermediate water are shown in figures 6.2 to 6.11.

The cross-sections show the measured values on the left side and the deviation calculated with M3 from the measured values on the right side. The deviations can be positive or negative, showing a gain or a loss in the system, due to reactions or biological processes. The results are compared with the suggested biological processes defined by Pedersen and Karlsson and are an attempt to understand and identify the processes governing the system in Bangombé.

Two data sets were used: the campaigns in 1993 and 1996.

The results of the mixing calculations for all observations are shown in Appendix 1.

M3 modelling results of the 1993 campaign

The M3 modelling results of the 1993 sampling campaign are presented in the following figures (figures 6.2 to 6.6).

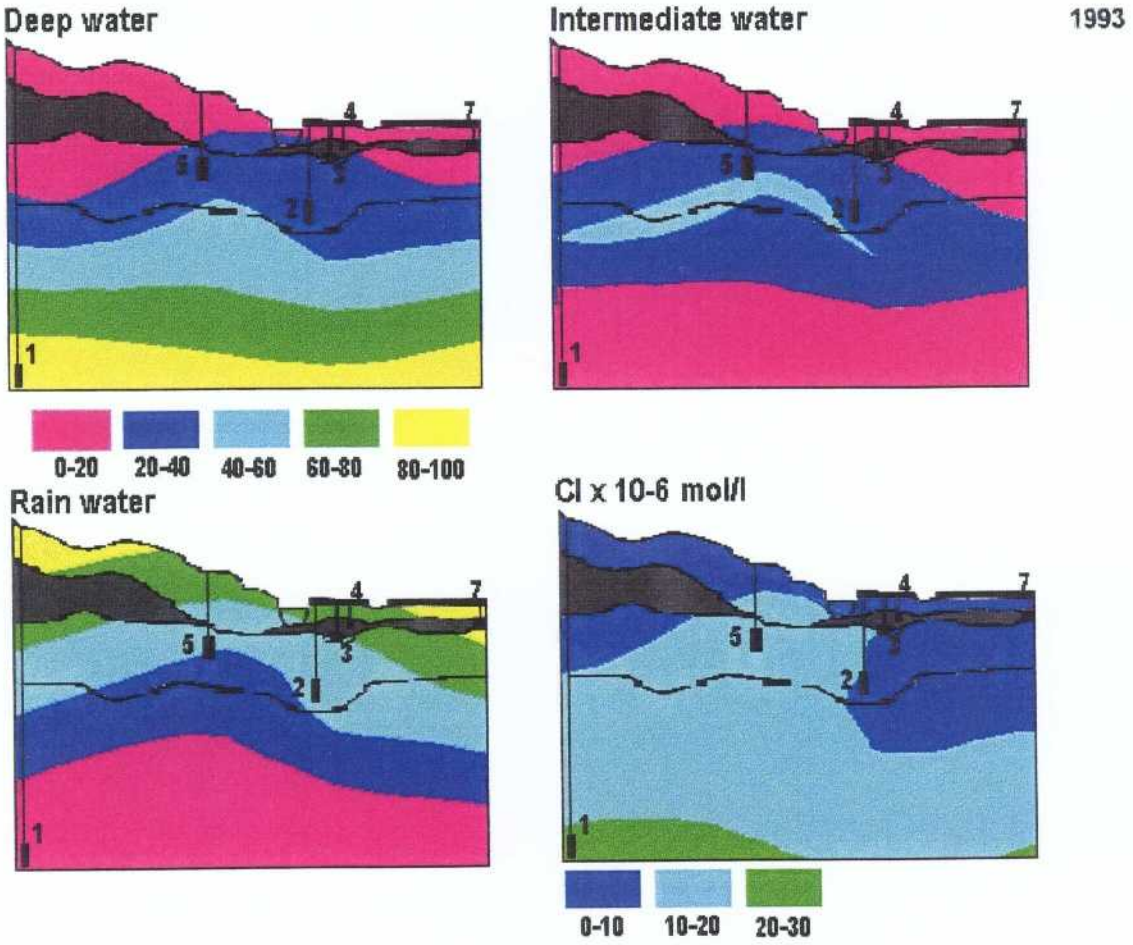

Figure 6.2 *Result of the M3 modelling of the rain, intermediate and deep waters (%), and the salinity distribution. Left picture measured values, right picture modelled values with M3. A high proportion of rain water is present at the surface of the model, decreasing towards the bottom. The deep water is present in a very small proportion at the surface, increasing towards the bottom where it is 100%. The salinity distribution shows the same tendency as the deep water distribution. A high proportion of intermediate water is present in the sandstones unit"a", which appear to be the highest permeable area of the system.*

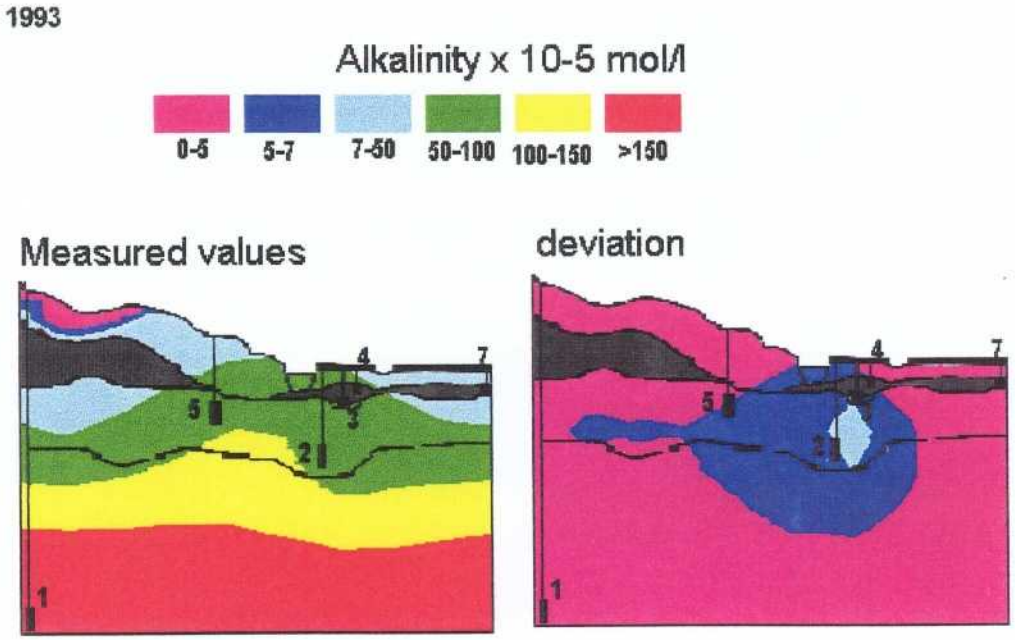

Figure 6.3 *Result of the M3 modelling of the alkalinity distribution in mol/l. Left picture measured values, right picture modelled values with M3. A positive deviation from the measured values is observed in the reactor zone. The increase of the alkalinity could be produced by the biological process generated by the organic matter (see Table 1). This assumption is in agreement with the biological reactions proposed by Pedersen and Karlsson.*

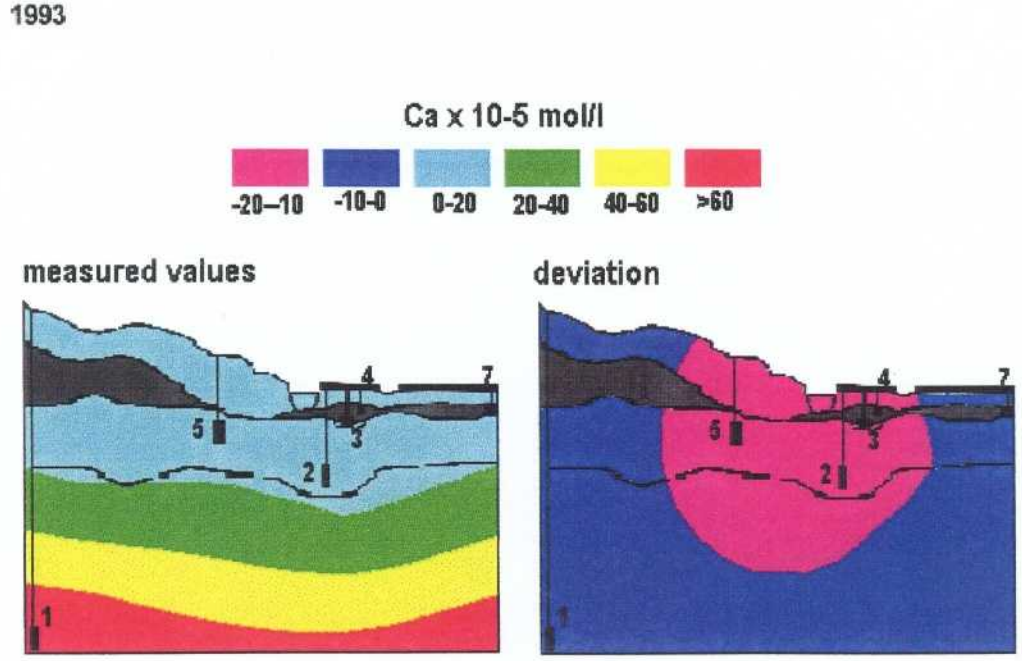

Figure 6.4 *Result of the M3 modelling of the calcium distribution in mol/l. Left picture measured values, right picture modelled values with M3. A negative deviation from the measured values is observed in the reactor zone. This may indicate that the increase of alkalinity in Figure 6.3 is not due to calcite dissolution. The increase of alkalinity by a decrease in calcium concentration, suggests that the increase in carbon dioxide from biological activity may have caused calcite to precipitate.*

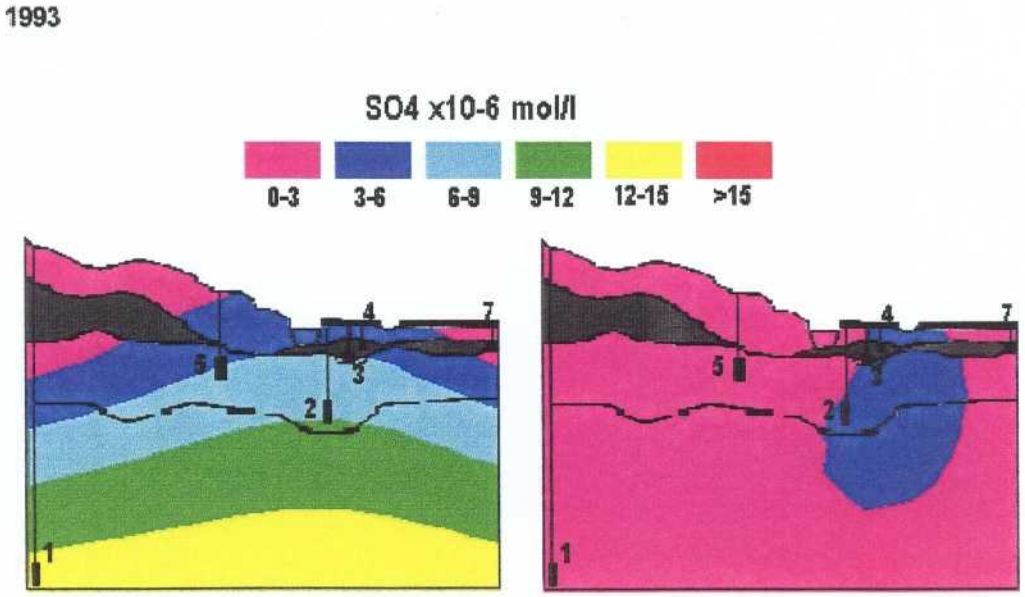

Figure 6.5 *Result of the M3 modelling of the sulphate distribution in mol/l. Left picture measured values, right picture modelled values with M3. A positive deviation from the measured values is observed in the reactor zone. Having a gain of sulphate, the third biological reaction proposed by Pedersen and Karlsson (see Table 1, sulphate reduction) can be excluded. The focus in the last field campaign was to identify the real biological mechanism, starting from these observations. The increase in sulphate in the vicinity of the reactor zone may be due to oxidation of S associated with the organic matter to sulphate, mediated by bacterial action.*

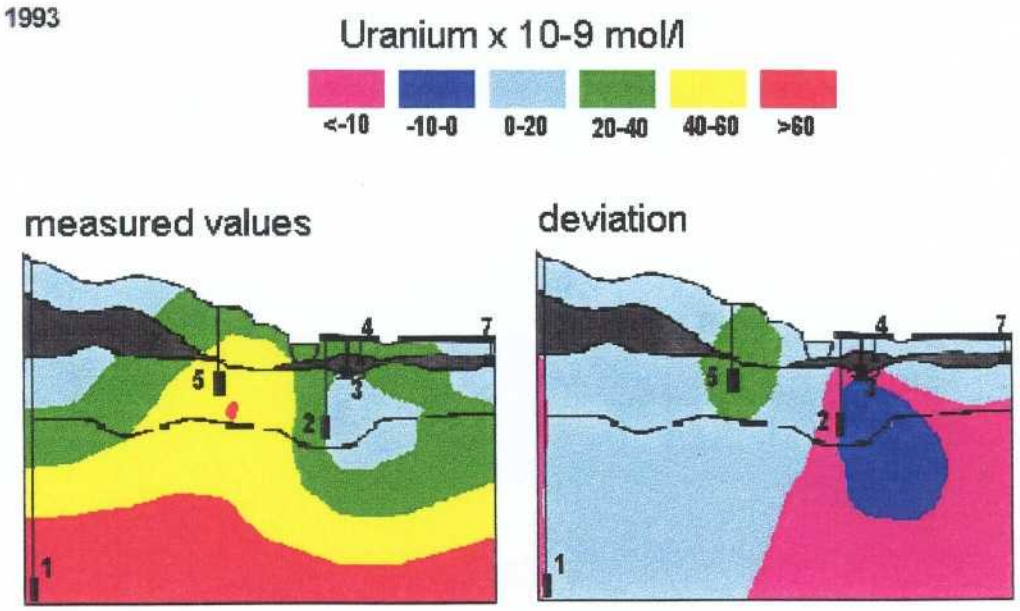

Figure 6.6 *Result of the M3 modelling of the uranium distribution in mol/l. Left picture measured values, right picture modelled values with M3. A negative deviation from the measured uranium values is observed in the reactor zone. The left half of the deviation plot shows a strange anomaly with high U concentration that disappears in 1996 sampling. A loss of uranium in the reactor zone is observed, showing no transport of uranium downstream the reactor. This result confirms the HYTEC-2D results (figure 5.2) of the existence of a buffer around the reactor zone protecting the uranium and avoiding the uranium transport.*

M3 modelling results of the 1996 campaign

The M3 modelling results of the 1996 sampling campaign are presented in the following figures (figures 6.7 to 6.11).

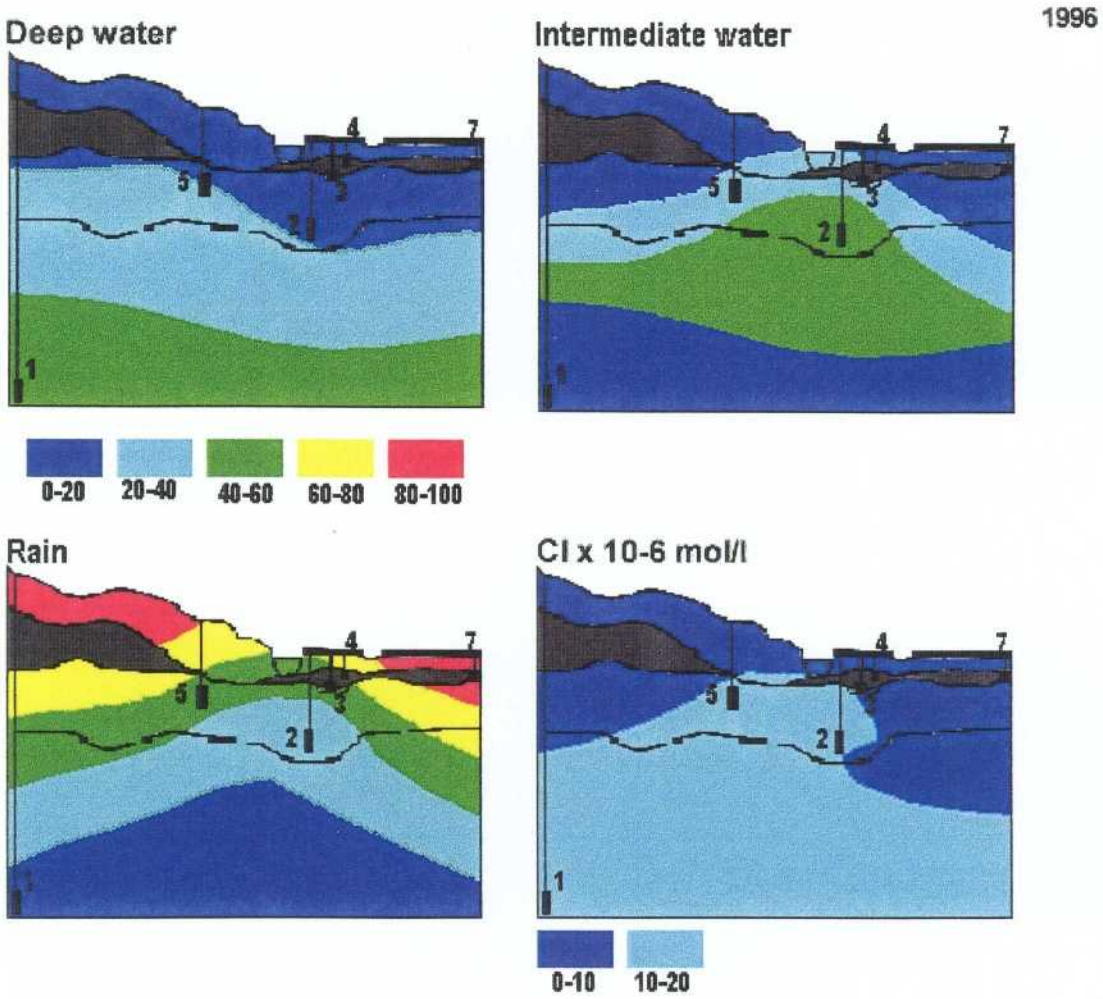

Figure 6.7 *Result of the M3 modelling of the rain, intermediate and deep waters (%), and the salinity distribution. Left picture measured values, right picture modelled values with M3. A high proportion of rain water is present at the surface of the model, decreasing towards the bottom. The deep water is present in a very small proportion at the surface, increasing towards the bottom. The rain water has displaced or diluted the previous deep water component to the extent of nearly equivalent in volume. The salinity distribution shows the same tendency as the deep water distribution. A high proportion of intermediate water is present in the sandstones unit"a", the principal aquifer of the system. In comparison with the 1993 campaign, the rain water is penetrating deeper in the system and more intermediate water is observed. These observations show a more disturbed, superficial system, where the superficial water penetrates deeper in the system and is flushed out quickly.*

1996

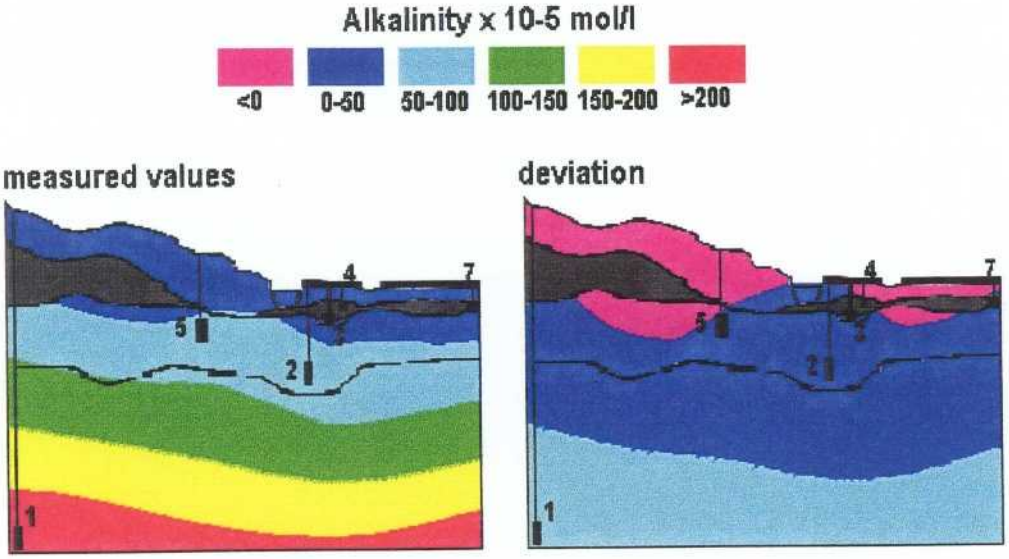

Figure 6.8. *Result of the M3 modelling of the alkalinity distribution in mol/l. Left picture measured values, right picture modelled values with M3. A positive deviation from the measured values is observed in all the sandstone unit "a" zone. The increase of the superficial water proportions induces a gain of alkalinity, further activating the biologic process generated by the organic matter. The gain in alkalinity is only at depth, especially in BAX01.*

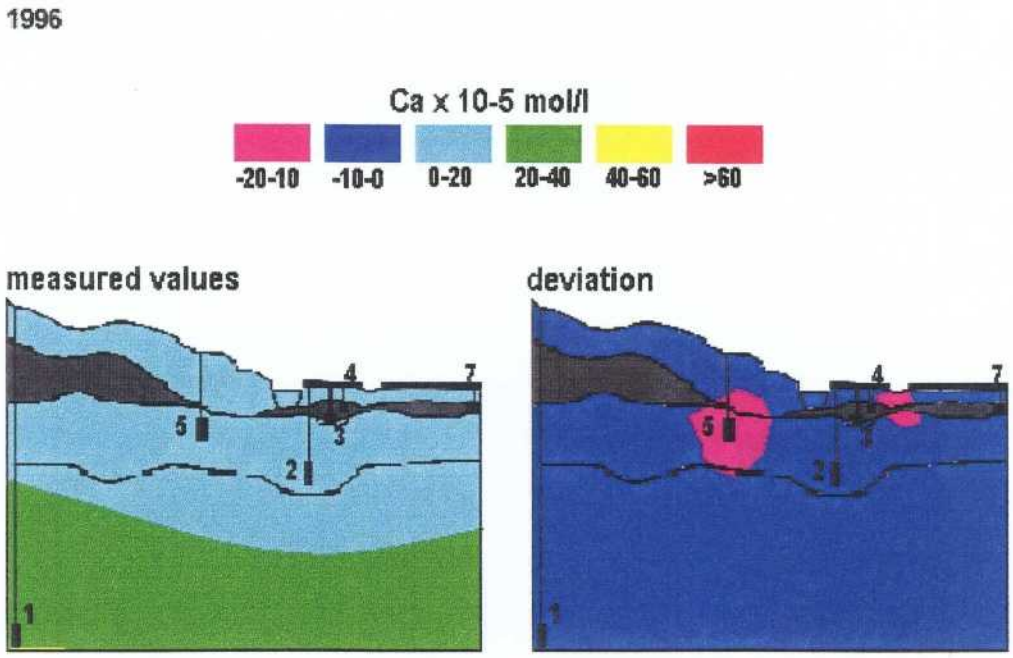

Figure 6.9 *Result of the M3 modelling of the calcium distribution in mol/l. Left picture measured values, right picture modelled values with M3. A negative deviation from the measured values is observed in a larger area then in 1993 (figure 6.4). This is in agreement with the assumption that the alkalinity is not a result from calcite dissolution.*

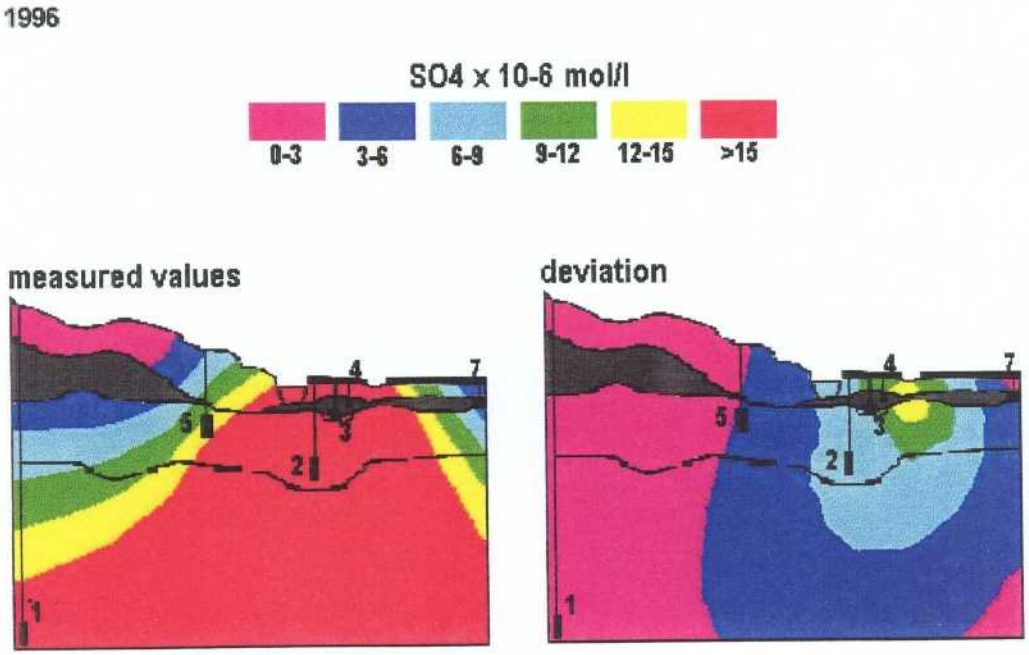

Figure 6.10 *Result of the M3 modelling of the sulphate distribution in mol/l. Left picture measured values, right picture modelled values with M3. A positive deviation from the measured values is observed downstream the reactor zone. The geochemical system is more superficial and is flushed out quickly. A transport downstream the reactor is observed. Sulphate is much higher than in 1993 samples, especially near the reactor zone and the surface. Perhaps rain water carries oxygen to the sulphur-rich zones, allowing bacteria to carry out more extensive oxidation of sulphur to sulphate.*

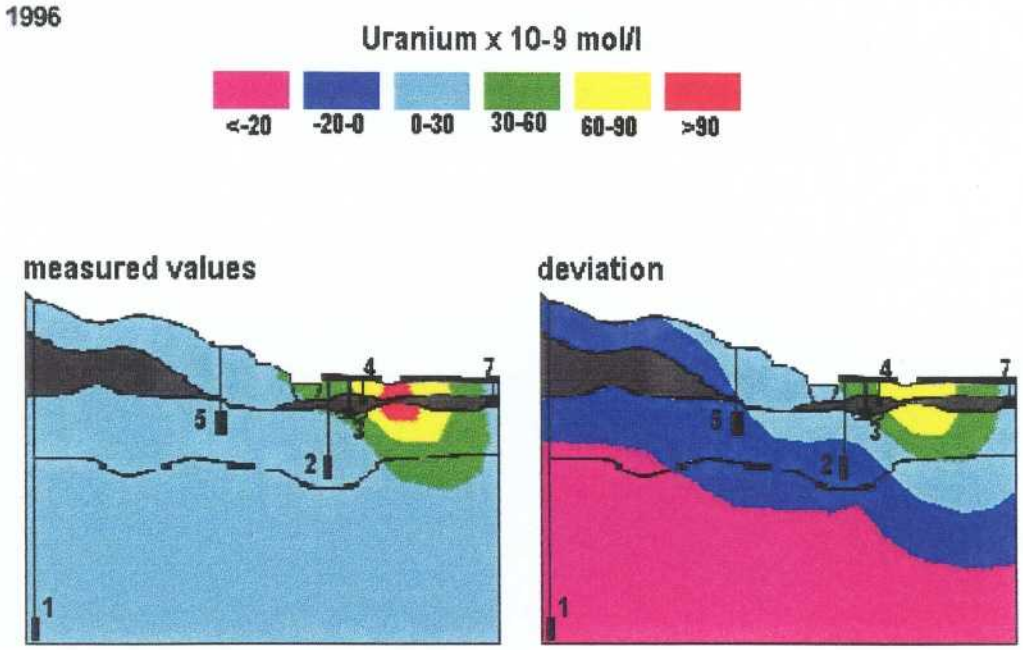

Figure 6.11 *Result of the M3 modelling of the uranium distribution in mol/l. A positive deviation from the measured uranium values is observed downstream from the reactor zone. In a superficial, disturbed system a transport of uranium is observed downstream from the reactor. The reactor zone does not show outward transport of U in 1993, so looks like the redox buffer contains U, in the 1996 plot there is transport outward (and upward) so the buffer is not acting as a trap.*

7 CONCLUSIONS OF THE COMPARISON BETWEEN HYTEC-2D AND M3

This exercise was in the beginning intended to represent a validation for M3, by comparing this statistic approach with the standard hydrodynamic- geochemical coupled code HYTEC-2D. It was realized that the codes complete each other and a better understanding of the geochemical studied system is obtained.

Thus, M3 can relatively easily be used to calculate mixing portions and to identify the sinks or the sources that may exist in a geochemical system. This can help to address the reactions in the coupled code such as HYTEC-2D, to identify the system and to reduce the computation time.

M3 shows the existence of the buffer around the reactor (sampling campaign 1993). No transport of uranium is seen downstream the reactor (see figure 6.6). HYTEC-2D gives the same result in the case when we consider the existence of the redox buffer (see figure 5.3) in the model.

M3 shows an increase of the alkalinity in the reactor zone (see figure 6.3).
This is showed also by the HYTEC-2D predictions which show an increase of the pH in the reactor zone, due to the existence of the buffer (see figure 5.2).

The HYTEC-2D and M3 modelling made for Bangombe indicated an existence of a chemical buffer around the reactor which may hinder the uranium transport. M3 modelling traced the effects from organic matter and iron reducing bacteria. This process was suggested to play an important role in regulating the redox conditions around the reactor. Any changes on the measured groundwater from sulphate reducing bacteria were not detected in the M3 modelling. During the last field campain (Karsten Pedersen et al. March, 1998) the microbes were sampled and identified in and around the reactor. Large amounts of iron reducing microbes, organic matter but no sulphate reducing microbes were detected at the Bagombe site. New *in situ* Eh measurements (D. Louvat personal communication 1998) indicated reducing conditions in the reactor zone. An important process adding reducing capacities and hindering uranium transport are therefore biogenic processes. The results from this field campaign support the above modelling presented in this study.

The above examples show the compatibility of the two different approaches. The two modelling approaches can be used to complete each other and to better understand the processes that can take place in nature. Thus, we can build confident tools which can be used for long term predictions of performance assessment.

8 ACKNOWLEDGEMENTS

This study has been supported and financed by the Swedish Nuclear and Waste Management Company (SKB). The helpful discussions and suggestions from Fred Karlsson (SKB), John Smellie (Conterra AB) and Virginia Oversby are acknowledged. Cecilia Andersson (INTERA KB) helped with finalizing the document. Izabella Halberg (Hallberg Translations) corrected the language.

REFERENCES

Bros, R., Gauthier-Lafaye, F., Samuel, J., Stille, P., (1993). Mineralogy and isotope geochemistry of clays associated with reactors at Oklo (reactor 10) and Bangombe. In: Oklo Working Group, Proc. of the third joint EC-CEA progress meeting, Bruxelles, 11-12 octobre 1993, p. 41-49.

Cordier, E., Goblet, P., (1996). Programme MÉTIS: Simulation d'écoulement et de transport miscible en milieu poreux et fracturé. Version 2.0. Notice d'emploi, CIG/EMP - LHM/RD/96/08.

Goblet, P., (1981). Modélisation des transferts de masse et d'énergie en aquifère, 1981, Ecole Nationale Supérieure des Mines de Paris - Université Pierre et Marie Curie.

Goblet, P., (1989). Programme METIS - Simulation d'ecoulement et de transport miscible en milieu poreux et fracture. Notice de conception au 9 fevrier 1989. Rapport EMP/CIG, LHM/RD/89/23.

Gurban, I., (1996). Caractérisation et modélisation de l'écoulement et du transport de matière au voisinage des réacteurs nucléaires naturels d'Oklo, Gabon, Thése de doctorat, Ecoles des Mines de Paris, Mémoires des Sciences de la Terre, Nr. 25, 194p.

Gurban, I., Ledoux, E., Made, B., Salignac, A.-L., Winberg, A., Smellie, J., Louvat, D., Toulhoat, P., (1996). Oklo, analogue naturel de stockage de déchets radioactifs (phase 1). Volume 3. Caractérisation et modélisation des migrations à distance des zones de réaction (sites d'Okélobondo et de Bangombé), Nuclear Science and Technology, Commision of the European Communities, Rapport Final.EUR Rep. 16857/3 FR, 177p.

Laaksoharju, M., Skårman, C., Skårman, E., 1998. Multivariate Mixing and Mass balance (M3) calculations, a new tool for decoding hydrogeochemical information. Submitted to Applied Geochemistry.

Laaksoharju, M., Wallin, B. (eds), 1997. Evolution of the groundwater chemistry at the Swedish Äspö Hardrock Laboratory site. Proceedings of the second Äspö international geochemistry workshop. SKB International Cooperation Report 97-04, Stockholm, Sweden.

Made, B., Salignac, A.-L., (1998). Modelisation couplee chimie-transport de la zone de reaction sur le site de Bangmbe (Oklo, Gabon). LHM/RD/98/4.

Nagy, B., (1993). Heterogenous composition and texture of the Oklo and Bangombe natural fission reactors. In: Oklo Working Group, Proc. of the third joint EC-CEA progress meeting, Bruxelles, 11-12 octobre 1993, p. 169-179.

Pedersen, K., Karlsson, F., (1995). Investigations of subterranean microorganisms. Their importance for performance assessment of radioactive waste disposal. SKB report 95-10, p. 222.

Salignac, A.-L., (1997). Programme STELE 2: Rapport final, Notice conceptuelle et d'utilisation du modèle HYTEC_2D, CIG/EMP - LHM/RD/97/12.

Salignac, A.-L., (1998). Étude du comportement des codes HYTEC sur des cas-tests d'oxydo-réduction. CIG/EMP - LHM/RD/98/8.

Toulhoat, P., Gallien, J.P., Louvat, D., Moulin, V., L'Henoret, P., Guerin, R., Ledoux, E., Gurban, I., Smellie, J.A., Winberg, A., (1994). Preliminary studies of groundwater flow and migration of uranium isotopes around the Oklo natural reactors. Fourth Inter. Conf. on the Chemistry and Migration behaviour of Actinides and Fission Products, Charleston, USA, p. 383-390.

Van der Lee, J., (1993). CHESS: another speciation and surface complexation computer code, Manuel, CIG/EMP - LHM/RD/93/39.

Van der Lee, J., (1997). Modélisation du comportement géochimique et du transport des radionucléides en présence de colloïdes, These, Ecole Nationale Supérieure des Mines de Paris.

APPENDIX 1: data used

Table 1: List of data used for the present modelling including the chemical composition and the calculated mixing portions.

	Rèf. échantillon	date prélèv.	Alk mole/l.	Cl mole/l.	SO4 mole/l.	Na mole/l.	K mole/l.	Ca mole/l.	Mg mole/l.	U mole/l.	Alk Deviation	Cl Deviation	SO4 Deviation	Na Deviation
3	BA120	Jun-91	2.18E-05	8.40E-06	5.50E-06	1.09E-05	3.60E-06	2.49E-06	1.60E-06	9.32E-09	-1.5E-05	1.8E-06	-1.6E-06	4.67E-07
4	BA121	Jun-91	4.96E-04	9.90E-06	4.50E-06	4.35E-05	1.46E-05	8.70E-06	1.52E-05	1.13E-09	0.000226	8.72E-07	-4.3E-06	-1.6E-05
5	BA122a	Jun-91	1.60E-03	5.90E-06	1.47E-05	3.83E-04	2.56E-05	4.60E-04	1.83E-04	5.63E-08				
6	BA122b	Jun-91	1.68E-03	7.10E-06	1.51E-05	3.83E-04	2.60E-05	4.80E-04	1.88E-04	7.94E-08				
1	BA142	Jun-91	1.64E-04	6.80E-06	1.34E-05	7.60E-05	7.20E-06	1.62E-05	2.10E-05	1.27E-08	1.6E-05	-2.4E-06	3.9E-06	4.08E-05
8	BA144	Jun-91	7.87E-04	1.02E-05	3.00E-05	1.60E-05	2.07E-05	1.37E-05	3.58E-05	2.33E-09	0.000578	-9.7E-06	9.16E-06	-4.1E-05
9	BA145	Jun-91	5.01E-04	9.30E-06	1.45E-05	2.80E-05	3.48E-05	1.37E-05	4.77E-05	8.85E-09	6.13E-05	-5.2E-06	4.24E-07	-7.1E-05
10	BA127	Mar-93	2.09E-04	8.74E-06	1.25E-05	1.78E-05	7.93E-06	2.25E-05	4.94E-05	4.62E-09	6.57E-05	-1.1E-06	2.27E-06	-1.7E-05
11	BAX01	Mar-93	2.51E-03	2.17E-05	1.35E-05	5.22E-04	5.37E-05	7.98E-04	2.10E-04	8.82E-08	0	0	0	0
12	BAX02	Mar-93	7.31E-04	4.23E-06	1.35E-05	3.48E-04	1.71E-05	8.98E-05	4.53E-05	1.76E-09	7.15E-05	-6.1E-06	4.91E-06	0.000209
13	BAX03	Mar-93	1.00E-03	1.30E-05	1.07E-05	5.22E-05	1.76E-05	9.98E-05	3.33E-04	1.34E-09	8.47E-05	2.5E-06	2.93E-06	-0.00014
14	BAX04	Mar-93	5.70E-04	8.74E-06	1.35E-05	3.65E-05	1.41E-05	4.74E-05	1.32E-04	4.62E-08	3.12E-05	-4.8E-07	5.6E-06	-7.7E-05
15	BAX05	Mar-93	1.08E-03	1.75E-05	1.25E-05	1.83E-04	2.56E-05	1.12E-04	1.60E-04	6.89E-08	5.29E-05	3.01E-06	8.43E-07	-3.4E-05
16	BAX03	Jul-94	4.41E-04	2.25E-06	2.03E-05	3.17E-05	1.13E-05	6.75E-05	2.48E-05	9.12E-09	0.00025	-8.2E-06	9.66E-06	-1.3E-05
17	BAX04	Jul-94	4.04E-04	3.66E-06	1.78E-05	1.35E-05	9.49E-06	3.53E-05	1.85E-04	1.11E-07				
18	BAX06	Jul-94	8.47E-04	1.72E-05	1.06E-05	1.61E-05	6.92E-06	4.13E-05	1.37E-04	1.18E-09	0.00044	4.01E-06	-2.2E-06	-7.5E-05
19	BA122	Jul-94	6.96E-04	6.98E-06	6.98E-06	1.14E-04	1.41E-05	1.85E-04	1.67E-04	1.48E-08	-6.1E-05	2.63E-07	2.69E-06	-4.2E-05
20	BAX01	Sep-96	2.36E-03	1.69E-05	1.77E-05	2.39E-04	2.95E-05	4.08E-04	1.65E-04	1.13E-08	0.000947	-3.2E-06	1.5E-06	-6E-05
21	BAX02	Aug-96	5.74E-04	8.17E-06	2.29E-05	2.65E-04	1.41E-05	9.25E-05	5.00E-05	2.31E-10	0.000116	-7.1E-06	8.04E-06	0.000162
22	BAX03	Aug-96	4.44E-04	1.30E-05	2.29E-05	1.52E-05	8.21E-06	2.10E-05	7.29E-05	1.30E-08	0.000277	-2.9E-06	6.26E-06	-3E-05
23	BAX04	Sep-96	4.92E-04	2.68E-06	2.19E-05	1.48E-05	6.15E-06	2.50E-05	9.17E-05	1.41E-07	-6.1E-05	-3E-06	1.79E-05	-9.9E-05
24	BAX05	Sep-96	7.70E-04	1.35E-05	1.88E-05	1.35E-04	1.36E-05	4.75E-05	1.04E-04	2.18E-08	0.00026	-1.6E-06	4.38E-06	2.19E-05
25	BAX06	Sep-96	1.84E-04	7.61E-06	2.92E-06	1.87E-05	1.10E-05	4.25E-05	1.88E-04	1.00E-09	-0.00027	3.07E-06	-2.2E-07	-7.5E-05
26	rain		1.33E-05	1.00E-12	1.00E-12	1.00E-12	1.00E-12	1.00E-12	1.00E-12	1.00E-12	0	0	0	0
27	surface		6.30E-05	2.28E-05	2.46E-05	2.98E-05	1.58E-05	2.30E-05	2.60E-05	7.73E-09	0	0	0	0

Blue=referencewater
Red+blue = used values in M3 calculations

	Rèf.	date	K	Ca	Mg	U	Mixing portions from M3		
	échantillon	prélèv.	Deviation	Deviation	Deviation	Deviation	Rain	Bax01	Intermediate
3	BA120	Jun-91	-1.11E-06	-7.01E-06	-6.6E-06	6.79E-09	71%	0%	29%
4	BA121	Jun-91	4.6E-06	-7.56E-05	-1.3E-05	-9.76E-09	60%	10%	30%
5	BA122a	Jun-91							
6	BA122b	Jun-91							
1	BA142	Jun-91	-1.01E-06	-2.94E-05	1.8E-06	5.79E-09	59%	5%	36%
8	BA144	Jun-91	4.51E-06	-5.47E-05	1.59E-06	-9.44E-09	12%	6%	81%
9	BA145	Jun-91	1.85E-05	-0.000126	1.28E-06	-9.1E-09	36%	16%	48%
10	BA127	Mar-93	-6.34E-07	-2.19E-05	2.99E-05	-2.31E-09	56%	4%	39%
11	BAX01	Mar-93	0	0	0	0	0%	100%	0%
12	BAX02	Mar-93	1.19E-07	-0.000118	-1.36E-05	-2.23E-08	54%	25%	21%
13	BAX03	Mar-93	-3.55E-06	-0.000189	0.000255	-3.12E-08	52%	36%	12%
14	BAX04	Mar-93	-2.66E-07	-0.000122	8.33E-05	2.64E-08	59%	21%	21%
15	BAX05	Mar-93	5.69E-08	-0.000214	6.92E-05	3.16E-08	35%	40%	25%
16	BAX03	Jul-94	1.62E-06	7.91E-06	1.18E-06	4.69E-10	54%	6%	40%
17	BAX04	Jul-94							
18	BAX06	Jul-94	-7.98E-06	-8.77E-05	9.43E-05	-1.53E-08	41%	15%	44%
19	BA122	Jul-94	-2.07E-06	-5.29E-05	0.000104	-1.16E-08	69%	30%	1%
20	BAX01	Sep-96	-5.83E-06	-4.18E-05	3.96E-05	-4.03E-08	9%	55%	35%
21	BAX02	Aug-96	-3.01E-06	-5.33E-05	1.41E-06	-1.85E-08	32%	17%	51%
22	BAX03	Aug-96	-4.67E-06	-3.28E-05	4.58E-05	3.68E-09	30%	5%	65%
23	BAX04	Sep-96	-6.08E-06	-0.000148	4.54E-05	1.22E-07	74%	22%	4%
24	BAX05	Sep-96	-4.18E-06	-0.000115	5.17E-05	1.39E-09	33%	19%	48%
25	BAX06	Sep-96	1.01E-06	-9.95E-05	0.00015	-1.49E-08	79%	18%	3%
26	rain		0	0	0	0	100%	0%	0%
27	surface		0	0	0	0	0%	0%	100%

List of SKB reports

Annual Reports

1977-78
TR 121
KBS Technical Reports 1 – 120
Summaries
Stockholm, May 1979

1979
TR 79-28
The KBS Annual Report 1979
KBS Technical Reports 79-01 – 79-27
Summaries
Stockholm, March 1980

1980
TR 80-26
The KBS Annual Report 1980
KBS Technical Reports 80-01 – 80-25
Summaries
Stockholm, March 1981

1981
TR 81-17
The KBS Annual Report 1981
KBS Technical Reports 81-01 – 81-16
Summaries
Stockholm, April 1982

1982
TR 82-28
The KBS Annual Report 1982
KBS Technical Reports 82-01 – 82-27
Summaries
Stockholm, July 1983

1983
TR 83-77
The KBS Annual Report 1983
KBS Technical Reports 83-01 – 83-76
Summaries
Stockholm, June 1984

1984
TR 85-01
Annual Research and Development Report 1984
Including Summaries of Technical Reports Issued during 1984. (Technical Reports 84-01 – 84-19)
Stockholm, June 1985

1985
TR 85-20
Annual Research and Development Report 1985
Including Summaries of Technical Reports Issued during 1985. (Technical Reports 85-01 – 85-19)
Stockholm, May 1986

1986
TR 86-31
SKB Annual Report 1986
Including Summaries of Technical Reports Issued during 1986
Stockholm, May 1987

1987
TR 87-33
SKB Annual Report 1987
Including Summaries of Technical Reports Issued during 1987
Stockholm, May 1988

1988
TR 88-32
SKB Annual Report 1988
Including Summaries of Technical Reports Issued during 1988
Stockholm, May 1989

1989
TR 89-40
SKB Annual Report 1989
Including Summaries of Technical Reports Issued during 1989
Stockholm, May 1990

1990
TR 90-46
SKB Annual Report 1990
Including Summaries of Technical Reports Issued during 1990
Stockholm, May 1991

1991
TR 91-64
SKB Annual Report 1991
Including Summaries of Technical Reports Issued during 1991
Stockholm, April 1992

1992
TR 92-46
SKB Annual Report 1992
Including Summaries of Technical Reports Issued during 1992
Stockholm, May 1993

1993
TR 93-34
SKB Annual Report 1993
Including Summaries of Technical Reports Issued during 1993
Stockholm, May 1994

1994

TR 94-33

SKB Annual Report 1994

Including Summaries of Technical Reports Issued during 1994

Stockholm, May 1995

1995

TR 95-37

SKB Annual Report 1995

Including Summaries of Technical Reports Issued during 1995

Stockholm, May 1996

1996

TR 96-25

SKB Annual Report 1996

Including Summaries of Technical Reports Issued during 1996

Stockholm, May 1997

List of SKB Technical Reports 1998

TR 98-01

Global thermo-mechanical effects from a KBS-3 type repository. Summary report

Eva Hakami, Stig-Olof Olofsson, Hossein Hakami, Jan Israelsson

Itasca Geomekanik AB, Stockholm, Sweden

April 1998

TR 98-02

Parameters of importance to determine during geoscientific site investigation

Johan Andersson[1], Karl-Erik Almén[2], Lars O Ericsson[3], Anders Fredriksson[4], Fred Karlsson[3], Roy Stanfors[5], Anders Ström[3]

[1] QuantiSci AB

[2] KEA GEO-Konsult AB

[3] SKB

[4] ADG Grundteknik KB

[5] Roy Stanfors Consulting AB

June 1998

TR 98-03

Summary of hydrochemical conditions at Aberg, Beberg and Ceberg

Marcus Laaksoharju, Iona Gurban, Christina Skårman

Intera KB

May 1998

TR 98-04

Maqarin Natural Analogue Study: Phase III

J A T Smellie (ed.)

Conterra AB

September 1998

TR 98-05

The Very Deep Hole Concept – Geoscientific appraisal of conditions at great depth

C Juhlin[1], T Wallroth[2], J Smellie[3], T Eliasson[4], C Ljunggren[5], B Leijon[3], J Beswick[6]

[1] Christopher Juhlin Consulting

[2] Bergab Consulting Geologists

[3] Conterra AB

[4] Geological Survey of Sweden

[5] Vattenfall Hydropower AB

[6] EDECO Petroleum Services Ltd.

June 1998